Long-Term Stability of ERS-2 and TOPEX Microwave Radiometer In-Flight Calibration

Laurence Eymard, Estelle Obligis, Ngan Tran, Fatima Karbou, and Michel Dedieu

***Abstract*—The microwave radiometers on altimeter missions are specified to provide the "wet" troposphere path delay with an uncertainty of 1 cm or lower, at the location of the altimeter footprint. The constraints on the calibration and stability of these instruments are therefore particularly stringent. The paper addresses the questions of long-term stability and absolute calibration of the National Aeronautics and Space Administration Topography Experiment (TOPEX) and European Space Agency European Remote Sensing 2 (ERS-2) radiometers over the entire range of brightness temperatures. Selecting the coldest measurements over ocean from the two radiometers, the drift of the TOPEX radiometer 18-GHz channel is confirmed to be about 0.2 K/year over the seven first years of the mission, and the one of the ERS-2 radiometer 23.8-GHz channel to be −0.2 K/year. The good stability of the other channels is confirmed (drift less than 0.04 K/year). The use of continental targets for analyzing the long-term drift is evaluated: the natural interannual variability prevents one from directly monitoring the drift of each channel, but the relative variation between two channels of the same instrument is found reliable. Over cold areas (Antarctic and Greenland plateau), results are consistent with the "cold ocean" analysis. Intercomparison of radiometer absolute calibrations is performed over the same continental area, leading to an anomalously high difference between channels 36.5 and 37 GHz of the ERS-2 and TOPEX radiometers, respectively, over "hot" targets (Sahara desert and Amazon forest). To quantify and analyze this difference, other radiometer measurements are analyzed over the Amazon forest, from the Special Sensor Microwave Imager (SSM/I) and the Advanced Microwave Sounding Unit (AMSU). Biases are confirmed for both TOPEX and ERS-2 radiometers by comparing brightness temperatures and derived surface emissivities: the TOPEX radiometer channels exhibit a negative bias with respect to SSM/I and AMSU-A, whereas the ERS-2 radiometer 36.5-GHz channel is positively biased, by several kelvin in brightness temperature in both cases. The method presented here could be used for controlling the in-flight calibration of any radiometer, and correct for remaining calibration errors after launch.**

***Index Terms*—Calibration, microwave radiometry, receiver stability, satellite.**

Manuscript received January 25, 2005; revised February 11, 2005. This work was supported in part by the Centre National d'Etudes Spatiales under Contract CNES/CLS 731/CNES/00/8435/00 and in part by the European Space Agency under Contract 16971/03/I-OL.

L. Eymard was with the Centre d'etude des Environnements Terrestre et Planetaire (CETP), 31520 Ramonville Saint-Agne, France. She is now with the Centre National de la Recherche Scientifique (CNRS), L'Institut Pierre-Simon Laplace (IPSL), Laboratoire d'Ocanographie et du Climat Expérimentations et Approches Numérique (LOCEAN), 75252 Paris, France (e-mail: Laurence.Eymard@lodyc.jussieu.fr).

E. Obligis and N. Tran are with the Collecte Localisation Satellites, 31520 Ramonville Saint-Agne, France.

M. Dedieu is with the Centre National de la Recherche Scientifique (CNRS), L'Institut Pierre-Simon Laplace (IPSL), 75252 Paris, France (e-mail michel.dedieu@cetp.ipsl.fr).

Digital Object Identifier 10.1109/TGRS.2005.846129

I. Introduction

THE MICROWAVE radiometers onboard altimeter satellites are specified to provide the "wet" troposphere path delay with an uncertainty of 1 cm or lower, at the location of the altimeter footprint. So any bias in the wet tropospheric correction directly impacts the sea level determination. They continuously measure the natural radiation from the atmosphere and surface at the vertical below the satellite. These instruments have two or three channels, including one in the water vapor absorption line centered at 22.235 GHz in order to properly retrieve the path delay [1], [2]. The quality of the retrieval relies on an accurate in-flight calibration, both in terms of absolute values and of time stability. To achieve this calibration, regular measurements of two known loads are performed, by switching the receiver either on an internal hot load (at ambient temperature) or on a sky horn, pointing to cold sky (cosmic background of 2.7 K and galactic noise). However, the microwave circuit is different for antenna measurement and for calibration, since switches are used to connect the receiver to the calibration targets (contrary to scanning radiometers, for which the calibration targets are seen during the antenna rotation). The on-ground calibration procedure, based on measurements in a thermal vacuum chamber, is not sufficient to ensure a good calibration, because: 1) the reflector is not generally included in the chamber, due to its diameter and 2) the temperature range does not correspond to space conditions, since the lower temperature is the one of liquid nitrogen (77 K).

Another source of calibration uncertainty is the antenna thermal environment: it is very difficult to properly estimate the radiation emitted by the various sources in space (including the satellite and the earth), even though a good characterization of the antenna pattern has been performed before launch. Finally the reflector quality is subject to degradation in space due to impacts with debris or other small particles.

For all these reasons, it is not possible to be fully confident in the prelaunch calibration adjustment, and careful analysis and correction is required after launch. Such analysis must moreover be repeated with time to ensure that no unknown effect has modified the instrument overall calibration.

In this paper, we compare the calibration of the microwave radiometers onboard the European Space Agency (ESA) European Remote Sensing Satellite (ERS-2) and the National Aeronautics and Space Administration Topography Experiment (TOPEX) for ocean circulation. The radiometer characterization and performance analysis of these radiometers was achieved through prelaunch ground calibration and in-flight calibration/validation [2]–[4].

TABLE I
MAIN CHARACTERISTICS OF THE ERS/ENVISAT AND TOPEX/JASON ALTIMETER MISSIONS, SSM/I AND AMSU-A MICROWAVE RADIOMETERS

MISSION	ERS1	TOPEX / TMR	ERS2 / EMWR	JASON1/JMR	ENVISAT	NOAA/ AMSU-A	DMSP/ SSM/I
Life in space	1991-1996	1992-	1995-	2001-	2002-	2000-	1987 -
Altimeter Frequencies (GHz)	13.8	TOPEX : 13.6 5.3 Poseidon : 13.6	13.8	13.575 5.3	13.575 3.2	—	—
Radiometer Channels (GHz)	23.8 36.5	18 21 37	23.8 36.5	18.7 23.8 34	23.8 36.5	23.8 31.4 50 (and oxygen absorption band) 89	18.7 22 37 89 (H and V except 22)
other information on measurements	Incidence angle +2.5 (23.8) and –1.5 (36.5) Footprint 20/22 km at 3dB	Nadir pointing – 21 and 37 GHz measurements interpolated on the 18 GHz footprint	Same as ERS1	Similar to TOPEX/TMR	Same as ERS1	Transverse scanning (7sec period) Nadir footprint size 40 km at 23.8 GHz	Comical scanning Footprint size 60 km at 18.7 GHz, 40 at 22, 25 km at 37 and 12.5 at 89 GHz
Orbit Inclination Cycle Node	Sun-synchronous 98° 35 days 10:30 desc.	62° 10 days	Sun-synch. 98° 35 days 10:30 desc.	62° 10 days	Sun-synch. 98° 35 days 10:30 desc.	Sun-synchronous 7:00 descending	Sun-synchronous 7:00 descending

After TOPEX launched in 1992, the TOPEX Microwave Radiometer (TMR) has continuously been operated without any major failure, and the retrieved wet tropospheric correction is still within the initial specifications. One year after launch, the ERS-2 Microwave Radiometer (EMWR) experienced an incident on one receiver, requiring a specific correction. Since this date, the radiometer performances have been slightly degraded (noise increase), but the wet tropospheric correction is still reliable and within the specifications. Comparisons of the two instruments were performed at cross-over points of the satellite orbits [5], showing small differences between their respective calibration in the current brightness temperature range over ocean, as well as in the retrieved wet tropospheric corrections. In 2000, several careful analyses of the TMR time series led to establish a weak drift of the radiometer along its life [6], [7].

The purpose of the present study is thus to examine the calibration of both radiometers and their variation along their life, using measurements over natural targets in the largest possible range of brightness temperatures. First, we apply a similar method to both instruments to determine the long-term drift in the coldest ocean brightness temperatures, then we investigate the usefulness of continental targets to evaluate the drifts at low and high temperatures. Finally, we propose a new method to compare the two radiometers at moderate and high brightness temperatures, based on surface emissivity retrieval, following [8] and [9].

Section II presents both radiometers and their known problems. In Section III, the "cold ocean" analysis is used to point out long-term trends on both instruments. In Section IV, the use of stable continental targets is evaluated in complement, to extend the brightness temperature range for drift analysis. Section V focuses on the comparison of absolute calibrations of both radiometers, and explores in more details the use of the Amazon forest as a "hot" target to intercalibrate microwave radiometers, by comparing brightness temperatures and derived surface emissivities. Finally, conclusions are summarized in Section VI.

II. IN-FLIGHT CALIBRATION OF THE ERS-2 AND TOPEX RADIOMETERS

A. Radiometer Specifications

To achieve a tropospheric correction uncertainty of one centimeter, the TMR as well as the JMR (Jason radiometer) both have three channels, one below the water vapor line at 18–19 GHz (low sensitivity to clouds), one in the absorption line (21–23.8 GHz) and one in the 30–40-GHz band (as sensitive to the surface as the low-frequency one, but more sensitive to cloud liquid water). The ESA ERS-1/2 and ENVISAT radiometers do not include the low-frequency channel. Due to this limitation, the wet tropospheric path delay retrieval is performed by using either the altimeter derived surface wind, or the backscattering coefficient in Ku-band as a "third" channel (see [10] and [11]). Table I summarizes the sensors and channels of the ERS-2/ENVISAT and TOPEX/JASON missions. Note that the ERS-1, ERS-2, and ENVISAT radiometers have the same specifications, and were calibrated in the same manner.

The major specificity of these radiometers is the Dicke switch: the gain stability is ensured by switching at a high rate (1 or 2 kHz) between the main antenna and a reference load, and the actual measurement is the difference between the Dicke reference load temperature and the antenna temperature. In consequence, the sensitivity to major calibration errors is reduced at high brightness temperature (close to the instrument

internal physical temperature) and maximal at low brightness temperature.

From on-ground calibration, the radiometer transfer functions (relation between the detected signal (voltage or digital count) and the brightness temperature) were established, and are used in the level 1 data processing (calibrated brightness temperatures) (see [1], [2], [4], and [12] for details concerning, respectively, ERS-1, ERS-2, and TOPEX radiometers). Measurements in a thermal vacuum chamber within a large range of temperature were used to establish a preliminary set of calibration coefficients for all microwave elements. The nonlinear response of the receivers with temperature was analyzed and corrected for [3]. Antenna pattern measurements were made in addition to complete the on-ground calibration. The absolute uncertainty was estimated from on-ground calibration, by evaluating all error sources within the radiometer (receiver, errors in loss coefficients, antenna characterization), and side lobe contribution errors, assuming they are not correlated (quadratic error of individual estimated errors in the case of ERS-1/2). For the three instruments, it was estimated to better or equal to ± 3 K. The radiometric sensitivity, derived from the time integration, bandwidth and noise temperature, was found to be lower or equal to 0.5 K (see [13] and [14] for more details about radiometer sensitivity).

After launch, the radiometer calibration of both instruments had to be tuned, leading to significant modification of some calibration coefficients, as any error in the characterization of microwave elements (loss factor, mainly) directly impacts the brightness temperature calculation. The resulting error increases with the temperature gradients within the radiometer and with the difference between the radiometer internal temperature and the input antenna temperature. For this reason, any drift in the calibration, due to degradation of a microwave component (as for example a switch loss) should have the largest effect at the lowest observed temperatures. Additional errors may come from inaccurate side lobe contribution estimates, which depend on the actual field of view of the antenna in orbit.

B. In-Flight Calibration: Methods and Results

For evaluating the in-flight calibration, the major difficulty is to find proper references. The methods currently used rely on the following comparison methods involving the instrument of interest:

—comparison with measurements from similar instruments;
—comparison with measurements from ground-based radiometers;
—comparison with simulations over sea using atmospheric profiles, sea surface temperature and wind, and a radiative transfer model;
—combination of the previous methods, by comparing simulations on the same meteorological fields with measurements from various other instruments (scanning radiometers as the Special Sensor Microwave/Imager SSM/I onboard the DMSP platforms or the TRMM Microwave Imager TMI. Main characteristics of these two instruments are given in Table I).

An additional indirect way to control the in-flight calibration is to validate the retrieved products, the path delay in this case. This can be achieved by comparing it to the path delay derived from operational radiosonde profile measurements over ocean (from ships, small islands), after selection of satellite data falling in a time space window centered on the radiosonde launch. Only noise is induced by collocation error, so any mean difference between path delays may be due to the calibration of the radiometer, to the radiosonde, or to the retrieval algorithm. An empirical adjustment may be performed afterward to fit the path delay with the required accuracy. Indeed, the radiosonde calibration uncertainty is a limitation for accurately determining the actual radiometer retrieval performance.

None of the above methods can ensure that brightness temperatures are calibrated with respect to an absolute reference, since the only observable reference is the "cold sky." The routine "cold sky" measurements are actually possibly biased by the errors on the thermal environment of the sky horn (or sky reflector). The use of such observations through the main antenna, by rotating the satellite, has occasionally been used for some radiometers. However this method ensures a good accuracy only for the lowest temperature, not for the whole range. Turning the satellite to look at the "cold sky" through the main antenna does not suppress any error, since the side lobe contributions come from the natural sources (sun, earth, etc.), which depend on the antenna view direction. Consequently, the calibration of a new radiometer has generally to be tuned to previous sensors considered as a reference (ENVISAT radiometer on ERS-2 one, itself calibrated on ERS-1 radiometer [4], [15], JMR on TMR as well, as done in [16]. Nevertheless the continuity between missions, even crucial for altimeter missions in the context of a sea level rise survey at the millimeter level, does not justify to neglect technological and algorithmic improvements and may lead to artificial calibration errors on new instruments.

Recent algorithmic improvements have been related to the development of powerful nonlinear statistical methods as neural network techniques [17]–[19], and the use of reliable radiative transfer models. Errors due to direct simulations are now very small for the atmosphere radiative transfer (in nonrainy conditions), allowing to properly simulate operational atmospheric sounders, like those onboard operational meteorological platforms [20]–[22]. Sea surface emissivity models are more questionable, since wave spectrum modeling is still an open issue, and only approximated electromagnetic scattering models are used (geometric optics, two-scale models). Although the accuracy of radiative transfer and emissivity models is subject to debate, the global error of brightness temperature simulations is probably lower than 5 K, from model comparison studies [22]–[24].

In the case of TMR, Ruf *et al.* [2] used a combination of various methods:

1) modeling the thermal behavior of the instrument as a function of internal temperature, as the solar heating had been found to impact the brightness temperatures by up to 10 K;
2) comparing measurements with those of ground-based radiometers and other water vapor measurements, as well as with SSM/I brightness temperatures over the Amazon forest; from these comparisons, biases on the three channels were evidenced;

3) reanalyzing and updating the on-ground calibration coefficient dataset, and adjusting the antenna pattern characterization (account for side lobe contributions) to reduce the observed biases.

The resulting final calibration uncertainty was estimated to range within ± 1.5 K. In addition, the retrieval algorithm was improved, to fine tuning the path delay retrieval. An increase of 8% of the strength of the water vapor absorption line in the model led to better fit radiosonde measurements [2].

For EMWR (the ERS-1 and ENVISAT microwave radiometers having the same specifications, in-flight calibration of all three was performed similarly), the in-flight calibration consisted of the following:

1) comparing brightness temperatures from ERS-2 with those of ERS-1 (which was on the same orbit, with an half an hour time lag during the first months of ERS-2 mission);
2) comparing measured brightness temperatures with simulated ones, using collocated profiles from the European Centre for Medium Range Weather Forecasting (ECMWF) model analyses. A space–time threshold of respectively $\pm 0.5^\circ$ and ± 30 min was taken, to statistically ensure that the same air mass is considered in both cases, and cloudy points were removed using cloud liquid water content predicted by the model and retrieved from EMWR using a retrieval algorithm [10], [15]. Any difference greater than 3 K (estimated calibration uncertainty) was then removed by tuning internal parameters controlling the in-flight calibration calculation (mainly the sky horn and the main antenna feed transmission coefficients) [1], [4], [15]. The relevance of this approach was evaluated by performing similar comparisons on several radiometers, with the same ECMWF analyses [23].

The estimated absolute calibration uncertainty was estimated to be equal or less than ± 3 K for EMWR.

The final validation of path delays was achieved using shipborne radiosonde profiles, and the uncertainties for TMR and EMWR were found to be less than 1 cm and about 1 cm, respectively.

C. Reported Calibration Anomalies

1) TMR: The TMR did not experienced any noticeable anomaly. However, the TMR developement was based on the Scanning Multichannel Microwave radiometer (SMMR) experience, which was flown onboard SEASAT and NIMBUS7 satellites. The SMMR calibration was found to anomalously vary, due to temperature changes in the antenna. To overcome this problem with the TMR, a radome was put to protect the main antenna and the sky horn, and a specific correction was applied [2]. Nevertheless, small brightness temperatures biases were found between measurements during two satellite yaw modes (fixed or sinusoidal). An empirical correction was proposed by Callahan [25].

Keihm *et al.* [26] pointed out a drift of the TMR wet tropospheric corrections with respect to SSM/I water vapor products and radiosonde measurements, and they concluded it was due to a -0.2 K/year drift in the 18-GHz TMR brightness temperatures. In Ruf, 2002, it was attributed to an increase of signal leakage from the warm calibration load to the radiometer antenna. More recent estimations of this drift show that it did not stop in 1996 as first suggested by Ruf *et al.* [16], but continued until 1998 [25].

2) EMWR: On June 16, 1996, a strong anomaly occurred on the 23.8-GHz channel. This anomaly was identified as a huge drop of the gain, which stabilized afterward at approximately one tenth of its original value, leading to a decrease of about 10 K in brightness temperature. This incident was identified as a possible failure of an amplifier in the receiver, and an empirical correction was proposed by [4] after fitting brightness temperatures over polar regions (characterized by large range of temperatures, and a weak day to day atmosphere variability) to those measured before the anomaly (just before and one year before).

[27] pointed out a possible drift of the brightness temperatures measured by the EMWR at 23.8 GHz by analyzing the difference between ERS-2 and TOPEX wet tropospheric corrections and brightness temperatures at cross-over points. The drift was confirmed and quantified later on [15], [28], [29]. The mean value for this drift was estimated to be -0.2 K/year corresponding to a wet tropospheric correction about 5 mm lower seven years after launch.

On both radiometers, the small trend detected could be due to aging effect on switches, as suggested by Ruf *et al.* [16] for TMR. Empirical functions depending on brightness temperature and time were proposed in [6] and [30] to correct for the respective drifts of each radiometer.

III. Long-Term Calibration Analysis of the Two Radiometers Over "Cold Ocean"

A. Coldest Brightness Temperatures Over Ocean

Several independent analyses established that the TOPEX radiometer (TMR) had drifted with time (implying a trend on the retrieved path delay). In 2000, [6] developed a method to evidence and monitor the drift of any of the three channels. Modeling considerations gave the order of magnitude of the minimum value, which could be measured over the ocean (cold water, specular reflection due to no wind and dry atmosphere conditions). A threshold was then derived from these values (minimum $+10$ K) to select data within each TOPEX cycle. The resulting brightness temperatures cumulative distribution histograms were then plotted and fitted with a third order polynomial function, that allowed extrapolation of the cold subset to the 0% occurrence brightness temperature value. Time series of these minimal temperatures for the three channels exhibited a significant difference between the 18-GHz channel and the others, confirming the drift on the 18-GHz channel. The obtained 18-GHz channel drift is 0.27 K per year over the first four years (end 1992 to end 1996), and a slightly lower rate since then. No significant drift was found on the other channels.

In Ruf's method [6], the three channels are processed independently, so the selected data from each channel used to derive the minimal temperature do not coincide in space and time. To check the possible importance of analyzing the same datasets for the three channels, we developed a method derived from

Ruf's one. Similarly, coldest measurements were first selected by keeping data below Ruf's lowest threshold +10 K, but for all channels together. Then the mean and standard deviation of the remaining data of each cycle were computed, and finally, only data falling below the mean minus 1.5 times the standard deviation, were considered. Thus an actual "coldest" dataset is kept within each cycle, instead of considering the extrapolated coldest possible value. The same method was applied to TMR and EMWR.

Fig. 1(a) and (b) show the results obtained for TMR and EMWR respectively. For TMR, Ruf's results are confirmed with a slightly lower trend: the 18-GHz trend is here of 0.20 K/year over the first seven years 1992–1999, and seems to decrease within the last two years (0.17 K/year when calculated over nine years). The trend change is observed in 1999, thus later than the date found by Ruf (beginning 1997). The 21-GHz channel is stable with time (0.02 K/year over seven or nine years) whereas a small trend is possibly significant on the 37-GHz channel (0.05 K/year over seven or nine years).

As for the TMR 18-GHz channel, the suspected EMWR 23.8-GHz channel drift is confirmed, the total decrease being −0.22 K/year over six years, whereas the 36.5 GHz has remained rather stable (0.04 K/year) over the same period. Note that the first year of ERS-2 radiometer data were not included in this analysis, because of the failure mentioned previously: any small error in the empirical correction of the gain drop was shown to induce artificial drift with respect to the first year. We analyzed the dataset linearly corrected for the reported gain anomaly.

B. Cross-Over Comparisons

The above method provided an accurate estimation of the drift for each channel, and the two radiometers were independently analyzed. An additional analysis was performed to compare TMR and EMWR drifts and their consequence on retrieved path delays on similar datasets, by using cross-over points between TOPEX and ERS-2 orbits. The TMR 21-GHz channel, identified as the most stable in the previous section, was taken as a reference to select the coldest points. A threshold of 134 K was applied to the 21-GHz brightness temperatures to select the lowest temperature data but providing reliable trends. Only those data, which were collocated with these selected 21-GHz brightness temperatures (1% of the total collocated data), were plotted. The collocation processing selects the EMWR and TMR closest measurement within a ±1 h common window around each orbit cross-over point. Fig. 2(a) and (b) shows the resulting plots for TMR and EMWR brightness temperatures at each frequency, respectively, and the trends are given in Table II. The trends are of the same order of magnitude but slightly different from those obtained with the previous method. This is mainly due to the dataset spatial distribution, since cross-over points between ERS-2 and TOPEX are mainly located at about 60° in latitude. The number of cross-over locations (a few hundreds) as well as their geographic distribution being limited, the uncertainty on the trend is higher than the one of coldest ocean data.

Fig. 3 shows the impact of the drifts on the ERS-2 and TOPEX wet tropospheric corrections at cross-over points. They

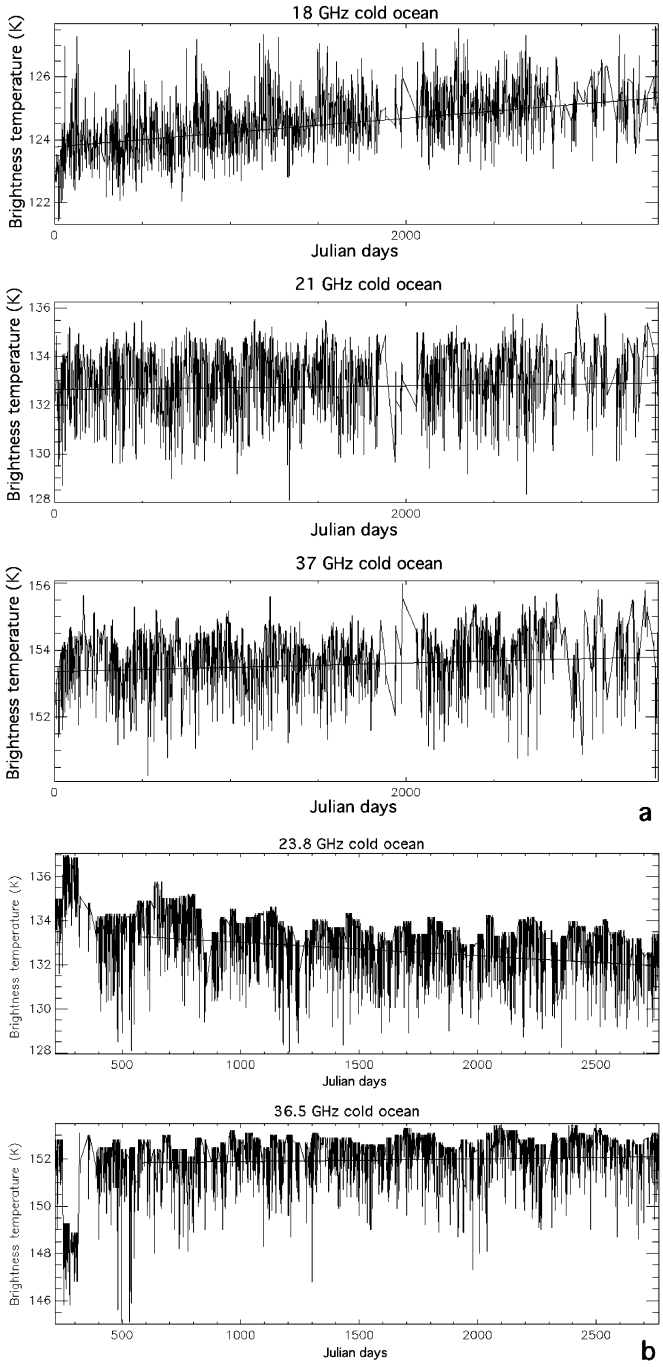

Fig. 1. Long-term monitoring of the coldest brightness temperatures (TB's) over the ocean for TMR and EMWR. Dates (in Julian days) are referenced to January 1, 1991. TB's are in Kelvin. Channels are labeled by their frequency (18, 21, and 37 GHz for TMR, 23.8 and 36.5 for EMWR). (a) TMR. The linear fit over the first seven years is superimposed. (b) EMWR. The linear fit over the last six years is superimposed.

both are less than 1 mm per year, showing that the two instruments are very stable over their life, despite their respective drifts.

C. Discussion

In Table II are also reported the drifts obtained by Ruf for the TMR 18-GHz channel, and by Scharroo *et al.* [29] using another method close to Ruf's one. In Scharroo *et al.*'s method,

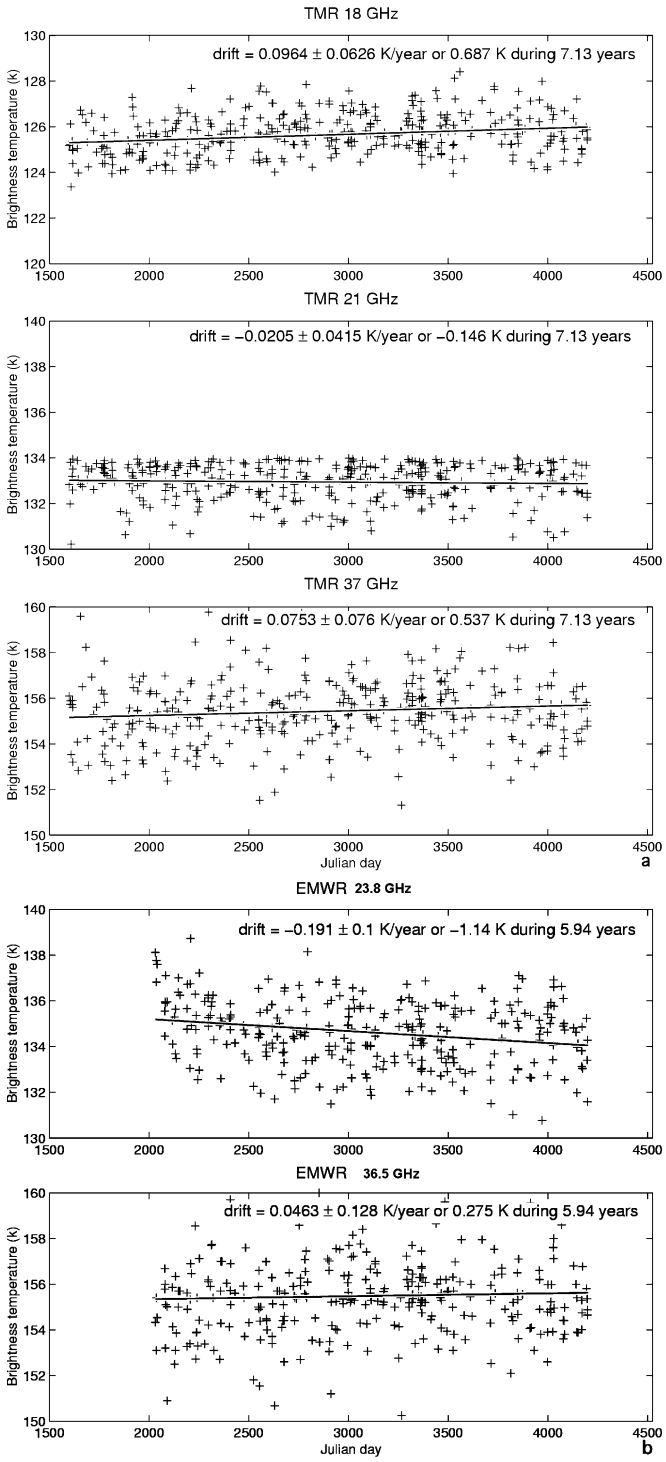

Fig. 2. (a) TMR and (b) EMWR brightness temperatures as a function of the julian day referenced to January 1, 1991. Selected pixels are cross-over points with ERS-2 for which TMR brightness temperatures at 21 GHz are lower than 134 K.

the coldest value of each cycle is derived from a linear extrapolation of the cold data histogram, taking the lowest 0.5 to 1% number of points.

For the TMR 18-GHz channel, the estimates of [6] and [29] and those from the two methods presented above are consistent and close to each other: the trend is 0.1 to 0.21 K/year over seven years, and it is 0.27 K/year over the four first years, from [6].

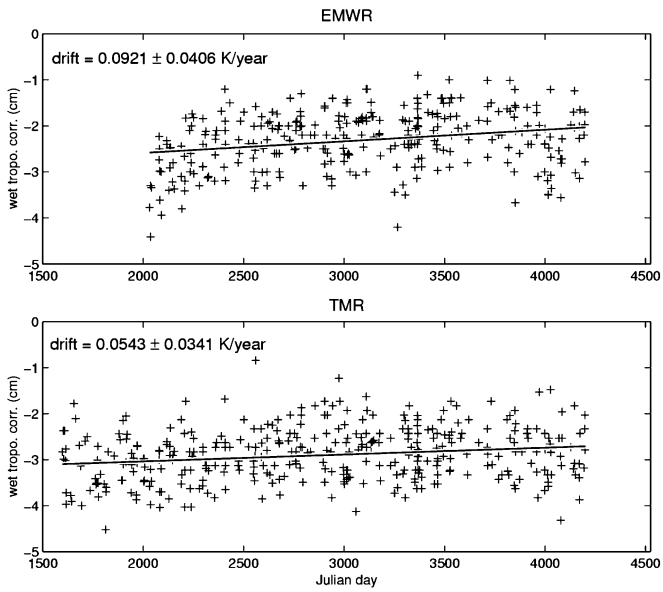

Fig. 3. Drift of the ERS-2 and TOPEX wet tropospheric correction, using cross-over points between the two missions and selecting the coldest TMR 21-GHz brightness temperatures over ocean.

TABLE II
TRENDS VALUES FOR THE TMR AND EMWR RADIOMETERS

Instrument	Channels (GHz)	Drift Cold Ocean (K/year)	Drift Cross-over (K/year)	Drift Scharroo et al(K/year)	Drift Ruf et al (K/year) over 4 years
TMR	18.0	0.20 ± 0.01	0.1±0.06	0.21	0.27
	21.0	0.02 ± 0.02	-0.02±0.04	0.03	-
	37.0	0.05 ± 0.01	0.08±0.08	0.02	-
EMWR	23.8	-0.22 ± 0.02	-0.2±0.1	-0.1	-
	36.5	0.04 ± 0.01	0.05±0.1	-	-

For the TMR the trends are estimated for a 7 years period, and for the EMWR for a 6 years period (except for the result from Ruf et al, 2000). The first column corresponds to the "cold ocean" method presented in section 3.1, the second one to selection of "cold" data on cross over locations (EWMR / TMR), the third refers to the study of Scharroo et al (2004), and the fourth to the study of TMR drift by Ruf et al, 2000.

For the two other channels, there is no drift estimate in Ruf's study, and the results obtained in the present study are consistent with [29]. They both conclude to very weak drifts on the 21- and 37-GHz channels. In view of the estimated error on the calculated trends, the 21- and 37-GHz channels may be considered as stable.

Concerning EWMR, consistent results on the 23.8-GHz channel are observed between our study and Scharroo's one (negative drift of about 0.1 to 0.22 K/year), whereas the 36.5-GHz channel trend is very weak. As for TMR, the latter channel may be considered as stable, in view of the estimated trend error.

As mentioned in Section II, the drifts evaluated at low temperature are the largest, so the average drift values at brightness

TABLE III
LOCATION OF TARGET AREAS FOR LONG-TERM SURVEY OF THE ERS-2 AND TOPEX RADIOMETERS. *ANTARCTIC PLATEAU IS NOT OVER-PASSED BY TOPEX

Area	South latitude	North latitude	West longitude	East longitude
Antarctic plateau*	-81.3	-81.0	114.0 E	116.0 E
Greenland plateau	65.0	66.0	47.0 W	43.0 W
Sahara desert	18.9	19.4	5.7W	4.8 W
Amazon forest	- 5.5	-4.5	67.0 W	64.5 W

temperatures usually measured over ocean are smaller. Consequently, the correction functions proposed by [30], [31], and [29] depend not only on time, but also on the brightness temperature magnitude.

IV. STABILITY ANALYSIS ON STABLE CONTINENTAL AREAS

In the previous section, the radiometer drifts were analyzed in the cold range of brightness temperatures, because no stable value can be found over ocean at higher temperature. To check the radiometer stability in a wider temperature range, we evaluate in this section the relevance of "hot" and "cold" continental targets. Continental areas are generally not used to check radiometer calibration, because of the high and very variable emissivity of the land surface. However, there are a few locations over the globe, where the atmosphere conditions and/or surface emissivity stability are sufficient to envisage such use. In this section, we test this approach to check the long-term stability of every channel at various temperatures.

A. Selection of Continental Targets

Criteria to select continental areas were the maximal horizontal homogeneity and a small time variability of the surface characteristics. The first year of ERS-2 radiometer measurements was explored, and various areas were investigated. Two "cold" and two "hot" areas were thus selected (see Table III). The first "cold" area is located over the Antarctic plateau, far from the coasts, close to the limit of the field of view of the EMWR due to the orbit inclination (82° in latitude), at an elevation of about 2000 m. It was chosen as the area with the coldest horizontally homogeneous brightness temperatures over the year. Weak snow falls occur each winter, and the wind is low. The second "cold" area is located on the Greenland plateau, as North as possible but within the TOPEX orbit overpass. The average brightness temperature is close to the mean value over ocean. One of the "hot" area is in the Sahara Desert (East Mauritania). The surface is very dry (no rain) and sandy. The last area is located in the Amazon forest, far from coasts and from mountains. Here the surface is covered with a dense vegetation, crossed by rivers.

These areas are small enough to assume horizontal homogeneity, except for specific elements which were removed (mainly a river in the northwest corner of the Amazon forest area), and they contain at least one orbital «« node »» of both missions.

All these areas, but the Amazon forest one, are characterized by a dry to very dry atmosphere throughout the year, so the brightness temperature time variations mainly come from surface temperature and surface emissivity variations. The Amazon forest was added because dense forest was shown to be the natural target which is the closest to a natural blackbody [2], [34]. In addition, the high mean temperature leads to a maximal emission in the microwaves, so the highest brightness temperatures over the globe. Over the four areas, we analyzed the long-term drifts of both radiometers.

B. Analysis Method

During each cycle, all EMWR and TMR data falling within the selected areas were taken. The EMWR time series (23.8-GHz channel) is plotted over each area on Fig. 4. Note that the EMWR first year was removed in the further data analysis, because of the bias induced by the imperfect correction of the anomaly (Section II). Before analyzing time series for each channel and each area, specific aspects, linked to the natural variations of the surface, had to be examined.

1) Diurnal Cycle: The diurnal cycle has an important effect over Sahara and Amazon forest. To take into account the variations of the surface temperature due to the diurnal cycle, the over-passing local solar time is considered. The Fig. 5 shows the average diurnal cycle of TMR brightness temperatures, over one year in the Amazon forest area. Contrary to the TOPEX mission, the ERS-2 one is in sun-synchronous orbit, crossing the equator at 10:30 A.M. and 10:30 P.M. (local solar time). TMR data were thus selected at the same overpass time as EMWR for each area, within ± 1 h. The difference between night and day temperatures made necessary to separate the corresponding overpasses over Sahara and Amazon forest.

2) Annual Cycle: The annual cycle strongly dominates the signal over Sahara and Antarctic areas. To evaluate the trend, an entire number of solar cycles was considered. As the solar cycle could mask other possible variability modes, a low-pass filter was also applied. Over the Antarctic plateau, an interannual variability was observed (period of about two years), which could influence the drift estimate.

3) Ice Melting: Over the Greenland area, the difficulty mainly comes from the huge variation of the brightness temperatures due to summer melting. The contaminated data were roughly eliminated by computing, for every annual cycle, the mean and standard deviation of brightness temperatures, then by removing those which are higher than the mean plus 0.5 times the standard deviation [see Fig. 4(b)]. This method is derived from the one developed by Torinesi *et al.* [32] to identify the melting signal on SSM/I data over the Antarctic coastal boundary.

C. TMR and EMWR Trends Over Continental Areas

Table IV summarizes the results of the EMWR survey over six years (after June 1996). Mean and RMS errors on the calculated trends are given. The first result is that the trends are different from an area to another, and that the RMS error is minimal over the Amazon forest, due to the weak annual cycle. Over the Antarctic plateau and Greenland, positive trends are found for both channels. Over Sahara and Amazon forest, the 23.8-GHz channel shows positive and negative trends, whereas the 36.5-GHz one presents a negative trend in every case. The

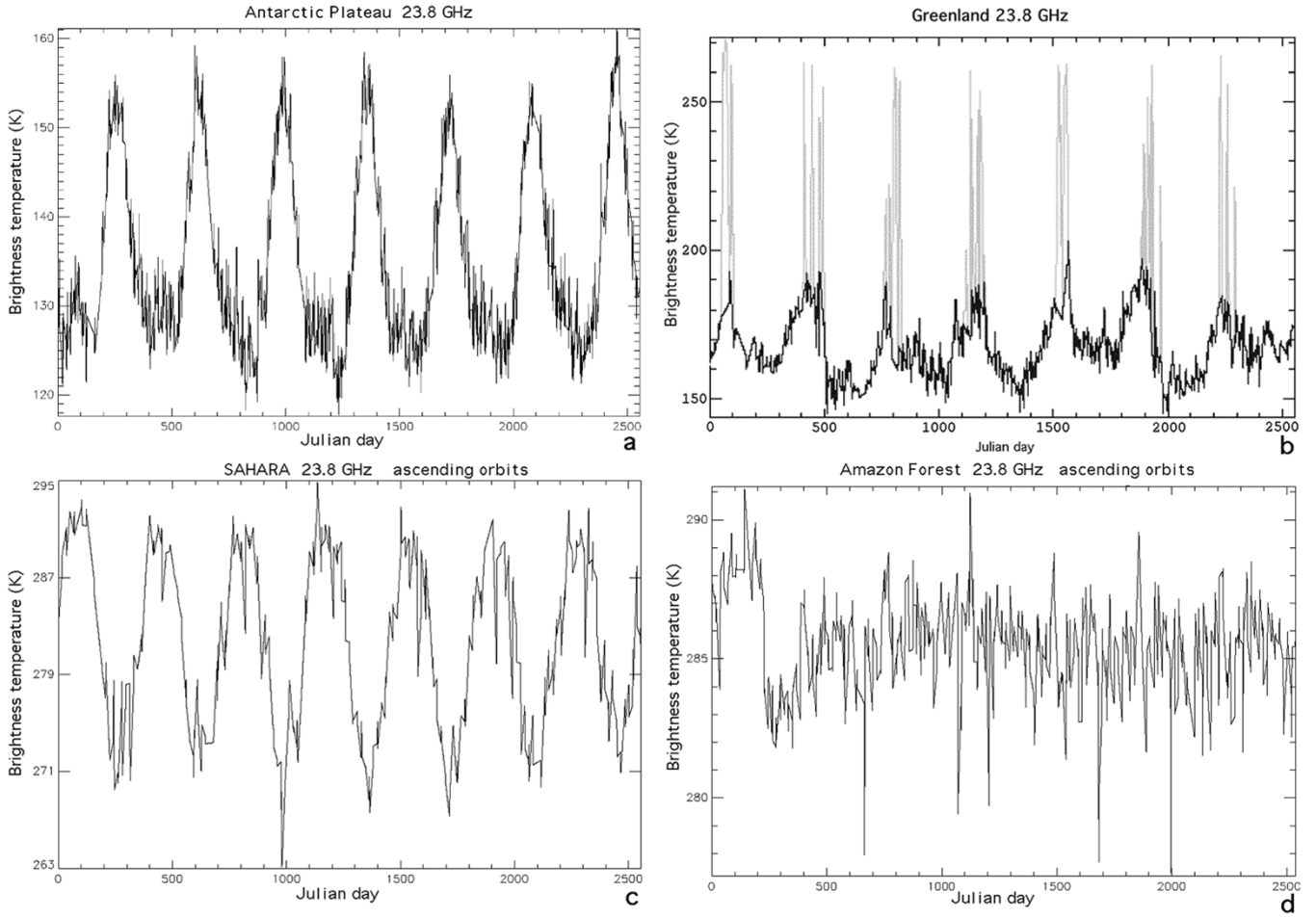

Fig. 4. Time series of EMWR 23.8-GHz channel over the four selected continental areas. (a) Coldest antarctic plateau. (b) Greenland. In this case, the original time series is in gray, and the selected data after removing the melting ice data are superimposed in black. (c) Sahara desert (ascending orbits). (d) Amazon forest (ascending orbits).

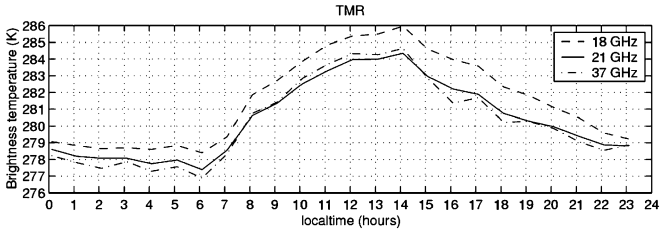

Fig. 5. Mean diurnal cycle of TOPEX brightness temperatures over the Amazon forest.

TABLE IV
LONG-TERM TRENDS OF THE EMWR TBS OVER STABLE CONTINENTAL AREAS FOR A SIX-YEAR PERIOD

Area	23.8 GHz (channel 1) K/year	36.5 GHz (channel 2) K/year	channel 2 – channel 1 trends* K/year
Antarctic	0.003 (0.199)	0.213 (0.165)	0.180 (0.081)
South Greenland	0.865 (0.176)	0.880 (0.199)	0.015 (0.233)
Sahara night	0.097 (0.116)	-0.053 (0.114)	-0.150 (0.050)
Sahara day	0.202 (0.113)	-0.036 (0.114)	-0.239 (0.046)
Amazon forest night	0.029 (0.024)	-0.082 (0.032)	-0.111 (0.041)
Amazon forest day	-0.107 (0.038)	-0.281 (0.043)	-0.173 (0.058)

* relative trend over the same duration for all areas.
RMS errors on the trends are given in parenthesis.

RMS error on the 36.5-GHz channel is small enough to assess the reliability of the trend, although it is slightly different for each time series. The natural interannual variation of each area is most likely the main cause of this discrepancy. However, the RMS error is reduced over Sahara and Antarctic areas by calculating the relative trend between the 36.5- and 23.8-GHz channels. Thus, by removing most of the natural variation of areas, reliable drift estimates are obtained: the trend is positive over the coldest target (Antarctic plateau), close to zero over Greenland, and it is negative over warm areas (Sahara and Amazon forest). The positive relative trend for the Antarctic area is consistent with the analysis over ocean (0.18 K/year, in agreement with the negative trend on the 23.8-GHz channel of -0.2 K/year over "cold" ocean). The result over "hot" targets (relative trend of about -0.16 K/year) suggests a possible drift of the 36.5-GHz channel (the 23.8-GHz channel does not present any noticeable variation, contrary to the 36.5-GHz one).

A similar analysis was performed on TMR data over nine years (Table V). Again, the RMS error on the trend is smaller for the Amazon forest than for the other areas, and it is significantly

TABLE V
LONG-TERM TRENDS OF THE TMR TBS OVER STABLE CONTINENTAL AREAS OVER NINE YEARS

Area	18 GHz	21 GHz	37 GHz
Greenland	0.302 (0.139)	0.256 (0.144)	0.275 (0.152)
Sahara night	0.244 (0.095)	0.230 (0.099)	0.267 (0.103)
Sahara day	0.197 (0.096)	0.163 (0.102)	0.190 (0.101)
Amazon forest night	0.050 0.051)	0.050 (0.055)	0.093 (0.036)
Amazon forest day	0.060 (0.024)	0.063 (0.018)	0.193 (0.028)
mean differences between channel trend (9 years) K/year			
Area		21-18 GHz	37 -21 GHz
Greenland		-0.046 (0.003)	0.019 (0.012)
Sahara night		-0.014 (0.001)	0.037 (0.002)
Sahara day		-0.033 (0.001)	0.027 (0.001)
Amazon forest night		+0.001 (0.009)	0.043 (0.005)
Amazon forest day		-0.003 (0.010)	0.130 (0.016)
RMS errors on the trend are given in parenthesis.			

TABLE VI
INTERCOMPARISON BETWEEN TMR AND EMWR MEAN BRIGHTNESS TEMPERATURES FOR EMWR OVERPASS TIMES

Area	TMR mean TBs over 9 years (K)			EMWR over 7 years (K)	
	18 GHz	21 GHz	37 GHz	23.8 GHz	36.5 GHz
Greenland	160.98	166.22	180.32	167.55	182.56
Sahara night	276.25	275.12	276.19	281.41	288.64
Sahara day	276.71	275.91	277.93	283.33	291.33
Amazon forest night	279.55	278.91	278.74	285.46	291.49
Amazon forest day	283.72	282.42	282.76	289.13	295.54

reduced when looking at the relative trends. Over Greenland, a slightly negative trend is observed for the relative trend between the 21- and 18-GHz channels (-0.05 K/year). It is qualitatively consistent with the 18-GHz drift observed over the "cold ocean," but weaker, as expected due to the higher temperature. The relative trends between the 21- and 18-GHz channels over the other areas are very weak, and of the order of magnitude of the RMS error. The relative trend between 37 and 21 GHz over "hot" targets is slightly positive. The magnitude of this trend is weaker than for EMWR channels, but probably significant, as the RMS error is small (0.06 K/year in average). A small drift of either the 21- or the 37-GHz channels could thus be possible.

Such drifts at high temperature were unexpected, because of the weaker sensitivity of the radiometer to calibration errors in this range. It might come from other parts of the instrument, as an amplifier. Although such drift has nearly no effect on the retrieved wet tropospheric correction, an accurate determination will be useful to characterize the instrument behavior in flight. However, to get more accurate estimates of these trends, it would be necessary to enlarge the "hot" areas to take into account a larger number of data within each cycle. The horizontal homogeneity of such larger area will have to be assessed, to ensure a low RMS error on the resulting trends. The best area would be the Amazon forest, because this forest is close to a blackbody, it is very stable with time, and the annual cycle is nearly negligible.

V. COMPARISON OF TMR AND EMWR ABSOLUTE CALIBRATIONS

A. EMWR-TMR Comparison of Mean Brightness Temperatures Over Continental Targets

The interest of selecting the same areas for TMR and EMWR is that a direct comparison of the measured brightness temperatures is possible, assuming that the surface emissivity does not significantly vary at frequencies close to each other. Estimates of the land surface emissivity using SSM/I [33] and AMSU-A [9] in the range 18–89 GHz validate this assumption. Consequently, in case the atmospheric absorption does not contribute for a large fraction in the measured brightness temperature, measurements at frequencies as close as 18, 21, and 23.8 GHz can be quantitatively compared, as well as measurements at 36.5 and 37 GHz. Table VI shows comparison results on the 3 selected areas, Greenland, Sahara and Amazon forest. Data are averaged over seven years for EMWR and nine years for TMR. In the following, we neglect the error due to the respective instrument drifts, considering the overall absolute calibration uncertainty (2–3 K).

The comparison between TMR and EMWR reveals a good agreement over Greenland (less than 2 K between the 21/23.8- and the 36.5/37-GHz channels), despite the slightly different frequencies. Over Sahara and Amazon forest, the difference between the 21- and 23.8-GHz channels is 6–7 K, and it is 12–13 K for 36.5/37-GHz channels. In view of the weak frequency difference, these differences are unexpected.

Over Greenland, brightness temperatures are in the range of those obtained over ocean. Most of the in-flight calibration and validation effort were made to optimize the data accuracy in this range. At high temperature, Ruf *et al.* [2] included comparisons with SSM/I, but on a limited dataset, and no calibration comparison was performed in this range for EMWR.

Contrary to low temperatures, for which modeling and path delay validation may be used to check the instrument absolute calibration, no method has been established yet to assess the calibration in the upper temperature range. The question that arose is which reference could we use to analyze the calibration of both sensors at high temperatures?

B. AMSU-A Brightness Temperatures as a Common Reference Over the Amazon Forest

To address this question, we chose to focus on the Amazon forest, as this deep forest is the closest to a natural blackbody for the microwave range, and presents a weak annual cycle, contrary to Sahara. This area presents small vertically and horizontally polarized TB difference (mean is approximately less than 1 K) as measured by the SSM/I radiometer at its two window channels at 19.35 and 37.0 GHz [34], which characterizes regions with high atmospheric opacity and an optically thick vegetation canopy. The measured TB's are weakly dependent on frequency (the surface temperature seen by the sensors is only slightly frequency dependent due to the difference in penetration depth into the medium). Nevertheless, the TOPEX and ERS-2 orbits do not

cross each other often enough to guarantee the statistical consistency of direct comparisons, except by averaging data over several years, as we did in the previous section. We could use SSM/I, as did [33], but this requires an empirical function for transposing measurements at 53° of incidence to nadir looking. Another scanning instrument of interest is AMSU-A.

AMSU-A provides a high spatial and temporal sampling of the earth's surface for a large range of frequency and has two channels (at 23.8 and 31.4 GHz) near those used on altimeter missions (see Table I). Moreover two field-of-view (fov) are at near nadir local zenith angle ($+1°40$ and $-1°40$) so the measurements are directly comparable with those of nadir viewing radiometers. AMSU-A is dedicated to temperature profiling through assimilation into weather forecasting models. AMSU-A onboard calibration is performed by scanning to the cold space background with the same antenna every 8 s for each scan line. Regarding these three items (regular complete internal calibration, two views close to the nadir point, frequencies near those of altimeter missions), the AMSU-A brightness temperatures can be considered as a reliable relative reference.

Nevertheless, the calibration assessment for each instrument has to account for contributions in the side lobes of the antenna before comparison of the brightness temperatures:

- —In SSM/I case, the incidence angle is constant but, within the antenna rotation, radiating elements such as a solar panel could bias the measurement for some scanning position. Corrections for the antenna side lobes were verified by aircraft underflights with an SSM/I simulator [2], making one confident on the SSM/I calibration over the Amazon forest.
- —For EMWR and TMR, contribution from the earth in the vicinity of the main lobe is assumed homogeneous and equal to the one in the main lobe. A 10° circle is taken for TMR, a 5° one for EMWR. Beyond this limit, for EMWR a fixed value is taken for the earth contribution, equal to the mean brightness temperature over the globe, whereas a value varying with latitude over ocean is taken for TMR (see [4] and [12]).
- —The AMSU-A transverse scanning reflector requires a careful analysis of the side lobe contributions with incidence angle, because contribution from the earth is maximal at nadir and decreases as the incidence angle increases up to the limb view. [35] proposed a calibration correction function of incidence angle. No information could be found on any surface type-dependent correction for AMSU-A.

When looking over the Amazon forest, far from the coasts, the difference between AMSU-A, SSM/I, TMR, and EMWR due to the various side lobe correction methods should be lower than 1 K, considering a 3% contribution and a temperature error of 20 K. We will therefore neglect it in the following.

C. Comparison of AMSU-A, TOPEX, and ERS-2 Brightness Temperatures Over the Amazon Forest

AMSU-A measurements for one full year, 2002, were used over the Amazon forest area (Table III). The scan pattern and geometric resolution correspond to a 40-km diameter 3-dB footprint at nadir. Since the NOAA-16 is in a circular sun-synchronous near-polar orbit, the selected area is over-flown twice a day at respectively around 02:00 local solar hour (LST) and 14:00 LST.

TABLE VII
AMSU-A BRIGHTNESS TEMPERATURES OVER THE AMAZON FOREST AREA

Nighttime	Mean and Standard Deviation (K)*				Number of points
	23.8 GHz		31.4 GHz		
Winter	286.0	1.1	283.1	1.5	185
Spring	285.5	1.0	282.2	1.4	163
Summer	285.5	0.9	282.3	1.1	155
Autumn	286.3	0.8	283.3	1.0	138
All year	285.8	1.0	282.7	1.4	641

Daytime	Mean and Standard Deviation (K)*				Number of points
	23.8 GHz		31.4 GHz		
Winter	290.9	2.1	288.5	2.3	107
Spring	290.5	2.0	288.1	2.2	106
Summer	290.3	1.5	287.9	1.7	111
Autumn	291.8	1.9	289.5	2.0	94
All year	290.9	1.9	288.5	2.1	418

*Mean and standard deviations were computed with the nighttime and daytime orbits respectively for the four seasons.

Measurements were taken during the daytime and nighttime passes to evaluate the stability of the brightness temperatures. Channels 23.8 and 31.4 GHz were studied, as they are the closest in frequency from TMR and EMWR ones. The brightness temperatures from FOVs number 15 and 16, closest to the nadir view, have average values greater than 280 K and standard deviations lower than 2 K, as summarized in Table VII. A small increase in the mean brightness temperature is evident from nighttime to daytime. Both nighttime and daytime values were found to have quite stable values over the four seasons. The variation over seasons and the standard deviations at night are slightly lower than those in the daytime hours. For this reason the nighttime data will serve as a reference over this area to compare the different sensor measurements.

We compared the brightness temperatures from TMR and EMWR versus AMSU-A. SSM/I data were also included for comparison with the previous study of [33]. We used their algorithm to recompute the SSM/I measurements into a vertical incidence configuration. We limited our comparison for TMR to time intervals close to AMSU-A overpasses. The SSM/I instrument on DMSP F-13 over-flies the area between 05:00 and 07:00 LST, and the ERS-2 one overpasses the area near 11:00 LST (A.M. and P.M.). Due to the different overpass time of the sun-synchronous satellites, we limited this comparison to nighttimes and early hours, to minimize the effect of the diurnal cycle: the differences could reach up to 4 K between dusk and dawn. A difference of 1–2 K would therefore be normal to observe between nighttime measurements of AMSU-A and ERS-2 ones, and a few tenths of kelvin between AMSU-A and SSM/I.

Average brightness temperatures over the nighttime hours are displayed in Table VIII. TMR exhibits the smallest values at all its frequencies. All reported 22–23.8-GHz measurements are in good agreement (AMSU-A, EMWR, and SSM/I extrapolated at nadir). The EMWR 36.5 GHz provides a too high value of 291.9 K. Except for the latter, we observed an overall slight decrease of brightness temperatures with increasing frequency. The standard deviation ranges between 1.0 and 2.8 K, giving a good confidence in the mean values.

TABLE VIII
MEAN AND STANDARD DEVIATION OF THE BRIGHTNESS TEMPERATURES OVER THE FREQUENCY RANGE FROM 18.0– 37.0 GHz AT NADIR AND FOR NIGHTTIME HOURS

	Mean and standard deviation (K)									
Frequency (GHz)	18.0	18.7	21.0	22	23.8	31.4	34.0	36.5	37.0	number
AMSU-A	-	-	-		285.8 (1.0)	282.7 (1.4)	-	-	-	641
TMR	278.6 (1.4)	-	278.1 (1.3)		-	-	-	-	277.6 (2.8)	2160
EMWR	-	-	-		285.7 (1.5)	-	-	291.9 (2.2)	-	3937
SSM/I	-	284.2 (1.3)	-	283.4 (1.6)		-	-	-	280.5 (2.4)	14564

External causes of discrepancy could be:

—the difference in frequency between channels compared (31–37 GHz, 18–23.8 GHz), but this would mean a significant difference in emissivity between these channels, in contradiction with results obtained in [8] and [9];

—differences in local measurement time, which can lead to 6-K variation, but was minimized by taking night hours only (less than 2-K variation). Effects of atmosphere variations (different atmosphere attenuation due to water vapor, clouds and rain) could also contribute to the discrepancy;

—horizontal heterogeneity of the area: the TMR and EMWR overpasses occur on specific portions of the area, different of each other, and possibly different from the global average, as seen by AMSU-A and SSM/I.

To further analyze this hypothesis, we must reduce the errors due to external factors. In Section V-D, we propose a new method, based on the calculation of the surface emissivity in each channel of each instrument, in order to remove most of these unknown external effects.

D. Comparison of Surface Emissivities

Prigent *et al.* [8] and Torinesi *et al.* [32] estimated the microwave land emissivity over the globe from SSM/I at the frequencies 19, 22, 35, and 85 GHz, for vertical and horizontal polarization, at 53 ° zenith angle by removing the atmosphere, clouds, and rain contributions using ancillary satellite data. The well-known simplified radiative transfer equation for one channel (stratified isothermal atmosphere) can be written as

$$\mathrm{TB} = T_{up} + T_s e\Gamma + (1-e)T_{down}\Gamma \qquad (1)$$

where TB is the measured brightness temperature, T_{up} is the upwelling radiation (from the atmosphere), T_{down} the downwelling radiation, including the galactic background G the atmosphere transmittance, T_s the surface temperature, and e its emissivity.

Providing T_s and atmosphere profiles, it is possible to derive e from TB measurements. Following a similar approach, [9] estimated the AMSU-A land surface emissivities for 30 observation incidence angles (from -58° to $+58^\circ$) and for the 23.8-, 31.4-, 50.3-, and 89-GHz channels, over January to August 2000. Collocated visible/infrared satellite measurements from ISCCP (International Satellite Cloud Climatology Project) were used to screen for clouds and to provide an accurate and independent estimate of the skin temperature [36]. The nearby temperature–humidity profiles from ECMWF Re-Analyses over 40 years (ERA-40) [37] were used as input to an updated radiative transfer model [38] in order to estimate the atmospheric contribution to the measured radiances. AMSU-A emissivity variations were analyzed as function of surface type, observation angle, and frequency. Surface types were identified using a surface classification [39] available at 30-km resolution. AMSU-A emissivities were also compared to SSM/I ones previously calculated by [33].

When sorted by observation zenith angle and by vegetation type, the AMSU-A emissivities show a significant angular dependence over bare soil areas. The emissivity angular and frequency dependence is found very weak over areas with high vegetation density. The deep forest emissivity was shown nearly constant with incidence with possibly a small decrease with frequency by 2% between 23.8 and 89 GHz. Moreover, a weak seasonal variability was found (less then 1%). For the 23.8- and 31.4-GHz channels, the emissivity calculations are as accurate as required for atmospheric applications: the day-to-day emissivity variation within a month is less than 2% (English [40] found that an accuracy of 2% is required for humidity profiles retrieval over land surfaces).

For AMSU-A, TMR and EMWR instruments, emissivity for each channel was calculated in a grid of 0.5×0.5 square degree meshes. At the studied frequencies, high thin ice clouds have a negligible impact on TB's observations. However, for an optimal accuracy of the emissivity estimates, only cloud-free data were selected for TMR and EMWR. The previously selected area in the Amazon forest was found too small to ensure a sufficient number of cloud-free observations over a short period of time (to reduce the seasonal variation impact). Consequently, this area was extended to the entire deep forest in South America. To select the deep forest area, the vegetation classification [39] was used. Among the 20 classes (including bare soil, crops, grass, various forest types, water bodies and several mixed cases), only the deep forest class (class 6—evergreen broadleaf trees) was considered.

Data from January 2000 were used for emissivity comparisons. For adequate comparisons between instruments, only AMSU-A data close to nadir (less than $\pm 10^\circ$ incidence) were taken.

AMSU-A mean emissivity maps over the Amazon forest as well as EMWR and TMR ones revealed geographical heterogeneities due to the rivers inside the forest (emissivity lower than the forest one). River data were removed from AMSU-A data using thresholds applied at each grid mesh on both mean emissivity and associated standard deviation (when a portion of orbit fails in the grid mesh, the variation due to a river leads to a higher standard deviation). The chosen minimum mean emissivity is 0.9, and the maximal standard deviation is 0.03. The remaining grid points were used for comparison with TMR and EMWR.

Fig. 6 shows the obtained maps after applying this selection. A residual "contamination" by rivers is likely in some locations. However, a negligible effect is expected on the average emissivity values. The AMSU-A standard deviation map looks slightly more "noisy" than those of EMWR and TMR. In the case of AMSU-A, cloud clearing was made by keeping clear air and cirrus clouds in the ISCCP classification. The cirrus class

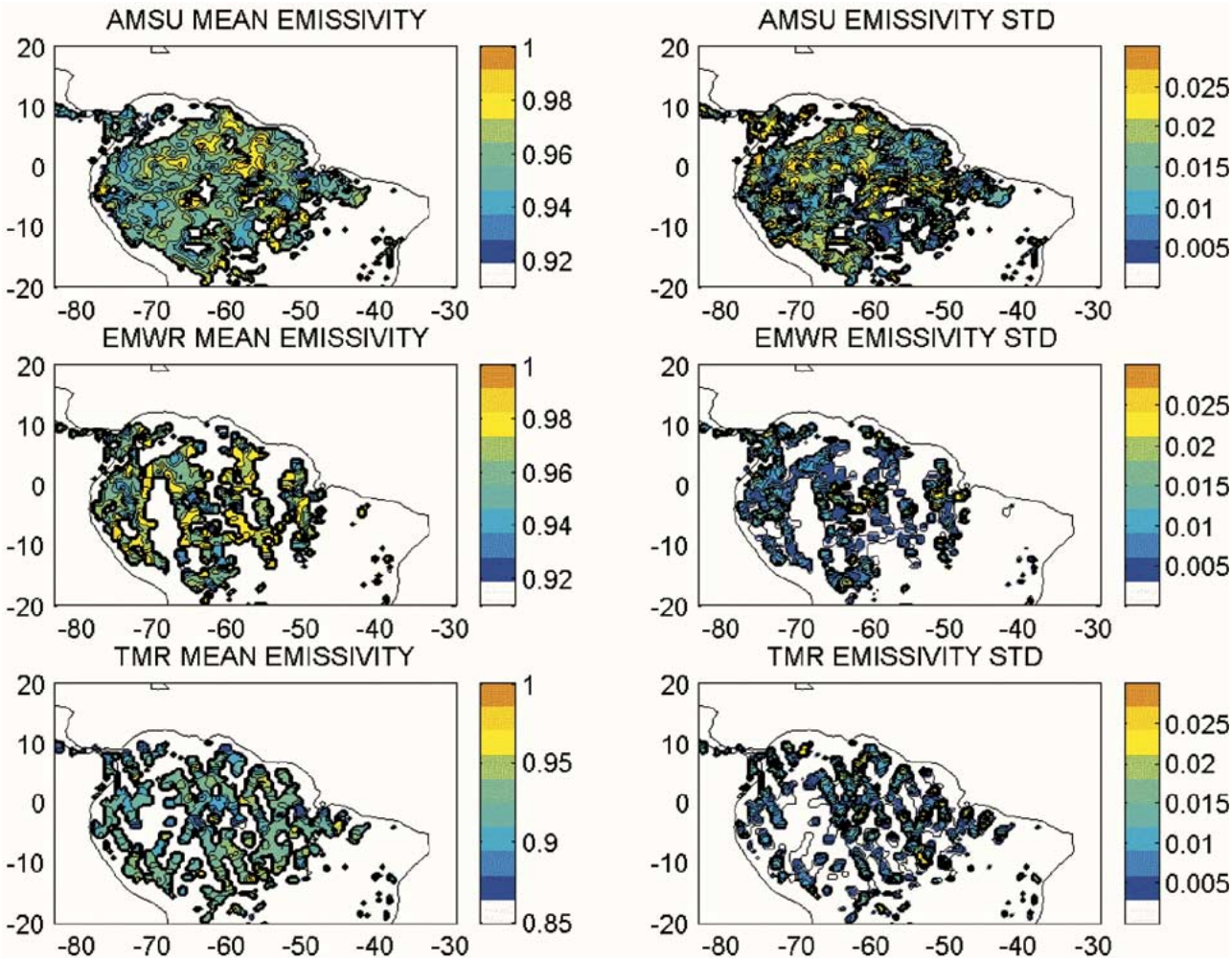

Fig. 6. Monthly mean maps (over January 2000), of the (top) AMSU-A 23.8-GHz, (middle) EMWR 23.8-GHz, and (bottom) TMR 21-GHz channels. The color scale is plotted at right of each map. (Left) Mean emissivity maps. (Right) Emissivity standard deviation. Maps are displayed on a regular grid of mesh 0.56◦ in longitude and latitude. Meshes for which the mean emissivity is lower than 0.9 and the standard deviation is greater than 0.03 were removed.

could include low clouds, which can affect the AMSU-A brightness temperatures due to absorption and scattering effects.

Before comparing the mean emissivities, three preliminary analyses were performed to check the reliability of emissivity calculations:

—emissivity distributions for the three instruments are similar and close to a Gaussian shape, except for a mean bias (not shown);

—the emissivity time evolution within the month (daily means computed over the area) is flat, with no standard deviation variation (not shown);

—the diurnal cycle (Fig. 7) exhibits a remaining variation for TMR, which is the only instrument for which emissivities are computed in the middle of the day and afternoon. The higher values obtained, compared with nighttime emissivities, suggest a likely bias in the day/night surface skin temperature or a wrong daily cycle of the ECMWF profiles.

Table IX gives the January averaged emissivities over the entire zone, as well as the associated standard deviations. SSM/I emissivities, as calculated by [8] are given for comparison. Due to the transverse scanning of AMSU-A reflector, comparison of AMSU-A and SSM/I data (at 533° incidence), requires combination of the SSM/I H and V polarization data to get the exact

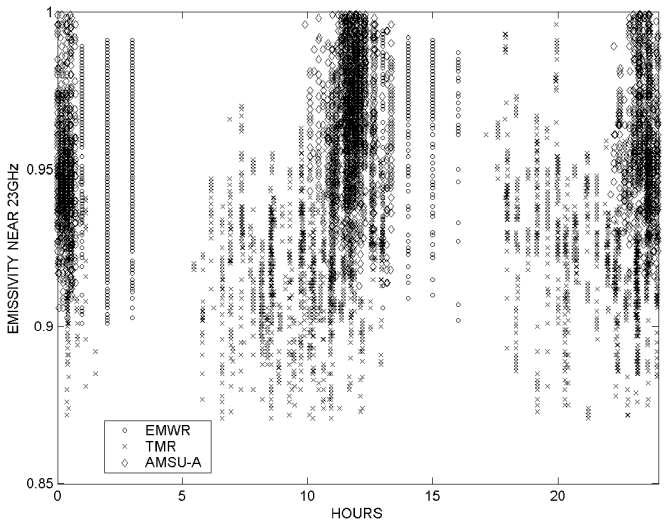

Fig. 7. Mean diurnal cycle of the retrieved emissivities at 21.0/23.8 GHz, over the month for the entire forest area. (Diamonds) AMSU-A. (Crosses) TMR. (Circles) EMWR.

AMSU-A one (there is no emissivity estimate for the 22-GHz channel, due to the unique V polarization). All standard deviations are close to 0.02, and the emissivities range between

TABLE IX
MEAN AND STANDARD DEVIATION OF THE EMISSIVITY OVER AMAZON FOREST FOR JANUARY 2000 FOR AMSU-A, TMR, EMWR, AND SSM/I CHANNELS IN THE 18–37-GHz RANGE

Frequncy (GHz)	18.7 and 19	21.0	23.8	31.4	36.5 and 37.0
AMSU-A		-	0.960 (0.020)	0.947 (0.019)	-
TMR	0.851 (0.023)	0.921 (0.022)	-	-	0.927 (0.022)
EMWR			0.962 (0.018)		0.974 (0.022)
SSM/I*	0.952	-	-	-	0.933

*The SSM/I emissivity at 22 GHz is not reported, because the calculation of the equivalent AMSU-A emissivity requires two polarizations.

0.85 and 0.97. AMSU-A and SSM/I emissivities are consistent within the 2% uncertainty, and they show a slight emissivity decrease with frequency as noted above (by 0.02 between 18.7 and 37 GHz).

With respect to the AMSU-A and SSM/I mean values, TMR emissivities are lower (particularly at 18 and 21 GHz), and the EMWR 36.5-GHz channel one is higher. For these channels (TMR 18/21 GHz and EMWR 36.5 GHz), the calculated emissivity differ by more than 2% from the mean AMSU-A value and this discrepancy is thus larger than expected from any external cause. In conclusion, comparisons over the Amazon forest both in brightness temperature and derived emissivity confirm the anomalous discrepancy between radiometers in the 21–37-GHz range.

The causes of this calibration discrepancy should be analyzed separately for each instrument. A first error source is the difference in side lobe contribution as mentioned in Section V-A, but this error cannot be responsible for more than 1-K discrepancy. In Section II, in-flight calibration methods for TMR and EMWR were compared. Brightness temperature comparisons and path delay validations were performed over open ocean, preferably in clear air. At high values, no efficient in-flight validation could be performed, because high temperatures over oceans are observed in deep clouds and over sea ice. Thus the temperature range of the in-flight calibration adjustment procedure was limited to the low–medium range of brightness temperatures. The procedure used by Ruf *et al.* [2] for adjusting the calibration in the high values consisted to fit TMR data to SSM/I measurements, after correcting the latter for incidence angle and frequency, based on modeling considerations. Concerning EMWR, [4] did not specifically adjust the high temperatures within the calibration correction procedure. The method used for tuning the in-flight calibration was indeed unable to correct for calibration anomalies at high temperature.

During on-ground calibration, the receiver response of each channel was analyzed, to check its linearity with the antenna temperature. However, the receiver linearity could not be checked on-ground between 3 and 77 K (the lowest temperature used), and there is no direct mean to assess the receiver linearity after launch. For TMR, on-ground calibration tests led to a slight parabolic response of the receivers, which was taken into account in the data processing [3]. Causes of the nonlinearity were not identified (amplifier gain response with temperature, leakage problem with a switch were two possible causes), but the resulting effect after launch is possibly related to the extrapolation of the gain modeled behavior to low temperature (down to 2.7 K instead of 77 K on-ground). Similarly, a slight nonlinear gain response with temperature was observed on EMWR during thermal-vacuum tests, and taken into account in the data processing. The observed EMWR anomaly suggests that either the receiver nonlinear response was not well enough corrected for, or that an unexpected perturbation occurred after launch (e.g., radio-frequency interference, as found by [41] on the U.K. Meteorological Office airborne radiometer). The slight decrease with time of the same channel (Table IV) could be related to the receiver degradation, supporting an internal receiver problem after launch. Recent studies of the Advanced Microwave Scanning Radiometer (AMSR) onboard the Japanese ADEOS2 platform and the AMSR for EOS (AMSR-E) onboard the USA AQUA satellite also suggest a receiver linearity problem to explain the anomalous biases between some AMSR channels and both SSM/I and the airborne AMR instrument over continents [42], [43].

As only indirect analyses of the instruments can be performed after launch, it is most likely that the exact calibration error cause will remain unknown. However, it will perhaps be possible to better characterize the calibration error as function of temperature by analyzing measurements over the widest possible range of brightness temperature, and looking at the internal temperature variations at day-night transitions and within the seasonal cycle.

VI. CONCLUSION AND PERSPECTIVES

In this study, we addressed the problems of the in-flight calibration of microwave radiometers over a large portion of their common life time, and over the whole temperature range. We compared TOPEX and ERS-2 radiometers over their common life time (seven years).

In a first step, we revisited Ruf's method for determining the long-term drift of TMR, by processing the three channels together, with a slightly simplified method. Consistent results were found, which confirmed the 18-GHz channel drift and showed the good stability of the 21-GHz channel. The same method, applied to EMWR, revealed a drift on the 23.8-GHz channel, but a good stability of the 36.5-GHz one. Cross-track comparisons confirmed again these results, and allowed to evaluate the drift impact on the wet tropospheric path delay in both cases. With respect to initial specifications, both radiometers are still compliant. However, these drifts must be compensated for to ensure the best accuracy, particularly for estimation of the long-term sea level variation. In both cases, a linear correction (function of time and temperature) has been proposed to date [29]–[31].

To enlarge the intercomparison of TMR and EMWR drifts, we examined the relevance of stable continental targets. On "cold" targets, as the Antarctic plateau and South Greenland, consistent trends were observed, but only in a relative manner (difference between brightness temperatures of two channels). They are consistent with the "cold ocean" drift analysis. Over "hot" targets, Sahara and Amazon forest, small drifts are suspected, but are unexplained.

In a second part, the absolute calibration of both radiometers were compared over stable continental areas. Over Greenland, measurements from TMR and EMWR were found consistent, within 2–3 K. However, "hot" targets revealed anomalously large differences between the two radiometers for both couples of frequencies (21/23.8 and 36.5/37 GHz). To further check the cause of this discrepancy, two successive comparisons were performed with AMSU-A and SSM/I corresponding channels. The advantage of AMSU-A is that its transverse scanning mode provides direct comparison at the same incidence angle with TMR and EMWR at nadir, and with SSM/I at 53°.

- A direct comparison of TMR, EMWR, AMSU-A and SSM/I brightness temperatures over one year for the same area in the Amazon forest evidenced a "warm" bias on the EMWR 36.5 GHz, and suggested a "cold" bias on TMR channels. But different orbit characteristics (overpass time) and external effects (diurnal cycle of surface and atmosphere variations) could be partly cause of these discrepancies;
- A comparison of derived land surface emissivities for the same channels was performed to remove all external error sources, using ancillary information from ISCCP for cloud clearing and surface temperature, and ECMWF reanalyses for atmosphere profiles. The "warm" bias on EMWR 36.5 GHz was again evidenced, with respect to SSM/I and AMSU-A derived emissivities. Looking at the frequency variation of emissivity (stable or slightly decreasing with frequency, from AMSU-A and SSM/I data) suggests that TMR 18 and 21 GHz are biased "cold," as the corresponding emissivity is about 3% lower than those of other sensors.

Such error in high brightness temperatures might be due to the in-flight calibration procedure, which generally relies on ocean data processing, thus in the low–medium range of brightness temperatures. It could also be due to a modified radiometer receiver response with temperature after launch with respect to on-ground calibration (nonlinearity of the receiver).

The use of stable continental targets is therefore complementary to "cold ocean," to validate the instrument in-flight calibration in the whole temperature range. It also allows one to compare measurements from different sensors, overpassing the same area, even at different times.

An area over the Greenland plateau was taken to compare the two radiometers over a "cold" target. The mean brightness temperatures over this area were found similar to ocean ones, but the trends were found less accurate than over other targets. Such an area is therefore of a limited interest for in-flight calibration.

The tropical forest appears as the most reliable target for such analysis, as it is the closest to a blackbody and has a weak annual cycle. So both the brightness temperatures and emissivities can be analyzed. The relative comparison of channels over Sahara showed results consistent with the Amazon forest. Desert areas could therefore be used in complement, but they require to overcome the problems of the strong annual cycle, and of the emissivity variations with incidence angle. It would be interesting to generalize this use of continental warm targets to systematically compare microwave radiometers after launch and monitor their drifts. Larger areas in tropical forests and deserts could be systematically used for analysis of high brightness temperatures and derived emissivities. They will not provide an absolute reference to which fit measurements, but a common relative reference. In complement to other methods, such method will ensure a better consistency of measurements from all microwave radiometers and check their calibration at high brightness temperatures.

ACKNOWLEDGMENT

The authors are grateful to the reviewers, who made fruitful suggestions for improving the paper. They thank A. Pilon, student at the Ecole Nationale Supérieure de Poitiers, in 2001, who helped in the development of the long-term drift analysis method.

REFERENCES

[1] R. Bernard, A. Le Cornec, L. Eymard, and L. Tabary, "The microwave radiometer aboard ERS-1, part 1: Characteristics and performances," *IEEE Trans. Geosci. Remote Sensing*, vol. 31, no. 5, pp. 1186–1198, Sep. 1993.

[2] C. Ruf, S. Keihm, B. Subramanya, and M. Janssen, "TOPEX/PSEIDON microwave radiometer performance and in-flight calibration," *J. Geophys. Res.*, vol. 99, no. 24, pp. 915-24–926, 1994.

[3] C. Ruf, S. Keihm, and M. A. Janssen, "TOPEX/poseidon microwave radiometer (TMR): I. Instrument description and antenna temperature calibration," *IEEE Trans. Geosci. and Remote Sensing*, vol. 33, no. 1, pp. 125–137, Jan. 1995.

[4] L. Eymard and S. A. Boukabara, "Calibration—Validation of the ERS2-2 Microwave Radiometer," ESA, Noordwijk, The Netherlands, Final Report of European Space Agency. Contract 11031/94/NL/CN, 1997.

[5] J. Stum, "Comparison of the brightness temperatures and water vapor path delays measured by the TOPEX, ERS-1 and ERS-2 microwave radiometers," *J. Atmos. Oceanic Technol.*, vol. 15, pp. 987–994, 1998.

[6] C. Ruf, "Detection of calibration drifts in spaceborne microwave radiometers using a vicarious cold reference," *IEEE Trans. Geosci. Remote Sens.*, vol. 38, no. 1, pp. 44–52, Jan. 2000.

[7] S. J. Keihm, V. Zlotnicki, and C. S. Ruf, "TOPEX microwave radiometer performance evaluation, 1992–1998," *IEEE Trans. Geosci. Remote Sens.*, vol. 38, no. 3, May 2000.

[8] C. Prigent, J.-P. Wigneron, W. B. Rossow, and J. R. Pardo-Carrion, "Frequency and angular variations of land surface microwave emissivities: Can we estimate SSM/T and AMSU emissivities from SSM/I emissivities?," *IEEE Trans. Geosci. Remote Sensing*, vol. 38, no. 5, pp. 2373–2386, Sep. 2000.

[9] F. Karbou, C. Prigent, L. Eymard, and J. Pardo, "Microwave land emissivity calculations using AMSU-A and AMSU-B measurements," *IEEE Trans. Geosci. Remote Sens.*, no. 5, May 2004.

[10] L. Eymard, L. Tabary, E. Gérard, A. Le Cornec, and S. A. Boukabara, "The microwave radiometer aboard ERS-1, part 2: Validation of the geophysical products," *IEEE Trans. Geosci. Remote Sensing*, vol. 34, no. 2, pp. 291–303, Mar. 1996.

[11] N. Tran, E. Obligis, and L. Eymard, "In-flight calibration/validation of ENVISAT microwave radiometer," in *Proc. IGARSS*, Toulouse, France, Jul. 2003.

[12] M. A. Janssen, C. S. Ruf, and S. J. Keihm, "TOPEX/Poseidon Microwave Radiometer (TMR): II. Antenna pattern correction and brightness temperature algorithm," *IEEE Trans. Geosci. Remote Sens.*, vol. 33, no. 1, pp. 138–146, Jan. 1994.

[13] F. T. Ulaby, R. K. Moore, and A. K. Fung, *Microwave Remote Sensing: Fundamentals and Radiometry*. Norwood, MA: Artech House, 1981, vol. 1.

[14] N. Skou, *Microwave Radiometer Systems: Design and Analysis*. Norwood, MA: Artech House, 1989.

[15] E. Obligis, N. Tran, and L. Eymard, "An assessment of Jason-1 microwave radiometer measurements and products," *Marine Geodesy*, vol. 27, pp. 255–277, 2004.

[16] C. Ruf, S. Brown, S. Keihm, and A. Kitiyakara, "JASON microwave radiometer: On orbit calibration, validation and performance," presented at the *Jason-1/TOPEX/Poseidon Science Working Team Meeting*, New Orleans, Oct. 21–23, 2002.

[17] V. M. Krasnopolsky, L. C. Breaker, and W. H. Gemmill, "A neural network as a nonlinear transfer function model for retrieving surface wind speeds from the special sensor microwave imager," *J. Geophys. Res.*, vol. 100, pp. 11 033–11 045, 1995.

[18] V. M. Krasnopolsky, "Neural networks as a generic tool for satellite retrieval algorithm development and for direct assimilation of satellite data," in *1st AMS Conf. Artificial Intelligence*, Phoenix, AZ, Jan. 11–16, 1998, pp. 45–49.
[19] S. Labroue and E. Obligis, "Neural network retrieval algorithms for the ENVISAT/MWR," ESA, Noordwijk, The Netherlands, ESA Rep. CLS/DOS/NT/03.669, 2003.
[20] E. Gérard and L. Eymard, "Remote sensing of integrated cloud liquid water: Development of algorithms and quality control," *Radio Sci.*, vol. 33, pp. 433–447, 1998.
[21] J. Pardo, C. Prigent, S. English, and P. Brunel, "Comparison of direct radiative transfer models in the 60 GHz O2 band with SSM/T-1 and MSU observations," presented at the *8th TOVS Conf.*, Auckland, New Zealand, 1995.
[22] L. Garand, D. S. Turner, M. Larocque, J. Bates, S. Boukabara, P. Brunel, F. Chevalier, G. Deblonde, R. Engelen, M. Hollingshead, D. Jackson, G. Jedlovec, J. Joiner, T. Kleespies, D. S. McKague, L. McMillin, J.-L. Moncet, J. R. Pardo, P. J. Rayer, E. Salathe, R. Saunders, N. A. Scott, P. V. Delst, and H. Woolf, "Radiance and Jacobian intercomparison of radiative transfer models applied to HIRS and AMSU channels," *J. Geophys. Res.*, vol. 106, pp. 24 017–24 031, 2001.
[23] L. Eymard, S. English, P. Sobieski, D. Lemaire, and E. Obligis, "Ocean surface emissivity modeling," C. Mätzler—UE COST and Univ. Bern, Brussels, Belgium, COST Action 712, 2000.
[24] W. J. Ellison, S. J. English, L. Lamkaouchi, A. Balana, E. Obligis, G. Deblonde, T. J. Hewison, P. Bauer, G. Kelly, and L. Eymard, "A comparison of ocean emissivity models using the advanced microwave sounding unit, the special sensor microwave imager, the TRMM microwave imager, and airborne radiometer observations," *J. Geophys. Res.*, vol. 108, no. D21, pp. 4663–4663, Nov. 2003.
[25] P. S. Callahan, "User notes for revised GDR correction product (GCPB)," Jet Propulsion Lab., California Inst. Technol., Pasadena, Tech. Note to the TOPEX/Poseidon/Jason Science Working Team, 2003.
[26] S. Keihm, M. Janssen, and C. Ruf, "TOPEX/POSEIDON Microwave Radiometer (TMR): III. Wet tropospheric correction and pre-launch error budget," *IEEE Trans. Geosci. Remote Sens.*, vol. 33, no. 1, pp. 147–161, Jan. 1995.
[27] J. Stum, F. Mertz, and J. Dorandeu, "Long-term monitoring of the OPR altimeter data quality,", Ifremer Contract no. 00/2.210 052, 2001.
[28] L. Eymard, A. Pilon, E. Obligis, and N. Tran, "Intercomparison of TMR and ERS/MWR calibrations and drifts," presented at the *Jason-1/TOPEX/Poseidon Science Working Team Meeting*, New Orleans, Oct. 21–23, 2002.
[29] R. Scharroo, J. Lillibridge, and W. Smith, "Cross-calibration and long-term monitoring of the microwave radiometers of ERS, TOPEX, GFO, Jason and ENVISAT," *Marine Geodesy*, vol. 27, pp. 279–297, 2004.
[30] E. Obligis, N. Tran, and L. Eymard, "ERS-2 drift evaluation and correction,", CLS/DOS/NT/03.688, 2003.
[31] C. S. Ruf, "Characterization and correction of a drift in calibration of the TOPEX microwave radiometer," *IEEE Trans. Geosci. Remote Sens.*, vol. 40, no. 2, pp. 509–511, Feb. 2002.
[32] O. Torinesi, M. Fily, and C. Genthon, "Variability and trends of the summer melt period of antarctic ice margins since 1980 from microwave sensors," *J. Clim.*, vol. 16, no. 7, pp. 1047–1060, 2003.
[33] C. Prigent, W. B. Rossow, and E. Matthews, "Microwave land surface emissivities estimated from SSM/I observations," *J. Geophys. Res.*, vol. 102, no. 21, pp. 867–21 890, 1997.
[34] S. Brown, C. Ruf, S. Keihm, and A. Kitayakara, "Jason microwave radiometer performance and on-orbit calibration," *Marine Geodesy*, vol. 27, pp. 199–220, 2004.
[35] T. Mo, "AMSU-A antenna pattern corrections," *IEEE Trans. Geosci. Remote Sens.*, vol. 37, no. 1, pp. 103–112, Jan. 1999.
[36] W. B. Rossow and R. A. Schiffer, "ISCCP cloud data products," *Bull. Amer. Meteorol. Soc*, vol. 72, pp. 2–20, 1991.
[37] The European Centre for Medium-range Weather Forecasts, Reading, U.K., 2000.
[38] J. Pardo, J. Cernicharo, and E. Serabyn, "Atmospheric transmission at microwave (ATM): An improved model for millimeter/submillimeter applications," *IEEE Trans. Antennas Propagat.*, vol. 49, no. 12, pp. 1683–1694, Dec. 2001.
[39] R. E. Dickinson, A. Henderson-Sellers, P.J. Kennedy, and M.F. Wilson, "Biosphere-atmosphere transfer scheme (BATS) for the NCAR community climate model,", Boulder, CO, NCAR Tech. Note NCAR/TN275+STR, 1986.
[40] S. English, "Estimation of temperature and humidity profile information from microwave radiances over different surface types," *J. Appl. Meteorol.*, vol. 38, pp. 1526–1541, 1999.
[41] A. McGrath and T. Hewison, "Measuring the accuracy of MARSS-an airborne microwave," *J. Atmos. Ocean. Technol.*, vol. 18, pp. 2003–2012, 2001.
[42] K. Imaoka, Y. Fujimoto, M. Kachi, T. Takeshima, T. Igarashi, T. Kawanishi, and A. Shibata, "Status of calibration and data evaluation of AMSR on board ADEOS-II," presented at the *SPIE Int. Symp. Remote Sensing Europe*, Barcelona, Spain, Sep. 8, 2003, [Online]. Available: http://sharaku.eorc.jaxa.jp/AMSR/data_re/amsr/index.htm.
[43] Y. Fujimoto, "Calibration status of the AMSR and AMSR-E," presented at the *Joint AMSR/AMSR-E Science Team Meeting*, Monterey, CA, Oct. 21–21, 2003, [Online]. Available: www.ghcc.msfc.nasa.gov/AMSR/monterey/Fujimoto_Calibration_Fujimoto.ppt.

Laurence Eymard graduated from Ecole Normale Superieure and Université Pierre et Marie Curie, Paris, France, in 1978. She received the Ph.D. degree in physics of the atmosphere in 1985.

She is currently a Senior Scientist (Directeur de Recherche) at the Centre National de la Recherche Scientifique (CNRS), Head of Laboratoire d'Ocanographie et du Climat Expérimentations et Approches Numériques (CNRS/IPSL/LOCEAN), Université Pierre et Marie Curie, Paris. Her Main research domains are atmosphere dynamics (boundary layer) and hydrological cycle, ocean—atmosphere interactions, and microwave radiometry. She coordinated experimental studies of the ocean–atmosphere interactions (SEMAPHORE, CATCH/FASTEX). She is principal investigator (PI) of the ERS/ENVISAT and Jason altimeter missions, and she is in charge of the in-flight calibration/validation of ERS microwave radiometers. She is also the PI of a new humidity sounder (SAPHIR) on the Megha/Tropique Indian French mission project to be launched in 2009.

Estelle Obligis received the Ph.D. degree in physics of remote sensing from the University of Paris VII, Paris, France, in 1996.

She joined the Collecte Localisation Satellites (CLS), Ramonville Saint-Agne, France, in 1998 and is currently in charge of the microwave radiometry activity. Her research has focused on the long-term survey of the ERS-2 radiometer, calibration/validation activity of TOPEX, Jason-1, and Envisat radiometers. She is also involved in studies dealing with SMOS, AltiKa, and Megha-Tropiques missions.

Ngan Tran received the Ph.D. degree in physical methods in remote sensing from the Université de Paris VI, Paris, France, in 1999. From 2000 to 2002, she was a Senior Scientist at the NASA Goddard Space Flight Center's Wallops Flight Facility for Raytheon ITSS. Since 2002, she has been at Collecte Localisation Satellites (CLS), Ramonville Saint-Agne, France. Her research interests are in the area of microwave remote sensing, both active and passive.

Fatima Karbou received the engineering degree in topography from the Institut Agronomique et Vétérinaire Hassan II, Rabat, Morocco, in 1999, and the Ph.D. degree in physics of remote sensing from Versailles Saint Quentin en Yvelines University, Vélizy, France, in 2004.

In September 2000 and during one year, she joined the ACRI research firm team at Sophia-Antipolis, France, as a Research Engineer. She worked on an air pollution simulator in both urban and rural environments and on NOAA instruments level 1 and two data processing tools. Her main fields of interest include the use of passive microwave instruments to estimate and analyze the land emissivities and to retrieve atmospheric parameters over land.

Michel Dedieu is ingenieer at the Centre National de la Recherche Scientifique (CNRS) and works in the L'Institut Pierre-Simon Laplace (IPSL) Centre d'étude des Environnements Terrestre et Planétaires (CETP), Vélizy, France. He has been working for ten years in data processing of space missions, both in the field of magnetosphere and earth observatin. He is in charge of the ERS-2/EMWR and ENVISAT/EMWR data monitoring chain in CETP, under ESA responsibility.